van Gunsteren, W. F., Berendsen, H. J. C., Geurtsen, R. G., & Zwinderman, H. R. J. (1986) *Ann. N.Y. Acad. Sci. 482*, 287–303.
Walberer, B. (1990) Simulationen zur Faltung von Proteinen, Master's Thesis, Technische Universität München.
Wang, A. H.-J., & Teng, M. K. (1990) *Crystallographic and Modeling Methods in Molecular Design* (Bugg, C. E., & Ealick, S. E., Eds.) pp 123–150, Springer-Verlag, New York.
Wang, A. H.-J., Cottens, S., Dervan, P. B., Yesinkowski, J. P., van der Marel, G. A., & van der Boom, J. H. (1989) *J. Biomol. Struct. Dyn. 7*, 101–117.
Weiner, S. J., Kollman, P. A., Nguyen, D. T., & Case, D. A. (1986) *J. Comput. Chem. 7*, 230–252.
Windemuth, A., & Schulten, K. (1990) *Molecular Simulation 5*, 353–361.
Wong, C. F., Zheng, C., & McCammon, J. A. (1989) *Biopolymers 154*, 151–154.
Zimmer, C., & Wahnert, U. (1986) *Prog. Biophys. Mol. Biol. 47*, 31–112.

Escherichia coli Glutaredoxin: Cloning and Overexpression, Thermodynamic Stability of the Oxidized and Reduced Forms, and Report of an N-Terminal Extended Species†

Victoria A. Sandberg, Betsy Kren, James A. Fuchs, and Clare Woodward*

Department of Biochemistry, University of Minnesota, St. Paul, Minnesota 55108

Received October 8, 1990; Revised Manuscript Received February 1, 1991

ABSTRACT: *Escherichia coli* glutaredoxin (MW 9700) catalyzes intracellular redox reactions utilizing a disulfide/dithiol enzymatic mechanism involving the active-site residues -Cys-Pro-Tyr-Cys-. It is functionally related to the thioredoxin family and is expected to share similar three-dimensional structure [Eklund, H., Cambillau, C., Sjöberg, B.-M., Holmgren, A., Jörnvall, H., Höög, J.-O., & Brändén, C.-I. (1984) *EMBO J. 3*, 1443–1449]. We constructed an overexpression system in which production of glutaredoxin is controlled by temperature-sensitive expression of the phage T7 promoter. In addition to glutaredoxin, a second gene product is observed; this species, which we call glutaredoxin N, is glutaredoxin extended by the sequence Met-Arg-Arg-Glu-Ile- at the N terminus. We have begun characterization of the structure and stability of the oxidized and reduced forms of glutaredoxin (grx-S_2 and grx-$(SH)_2$, respectively). Secondary structure calculated from CD data agrees with that predicted from the three-dimensional model of Eklund et al. The cooperative denaturation reactions of oxidized and reduced glutaredoxin were measured in temperature-induced and guanidine hydrochloride induced unfolding experiments. Surprisingly, oxidized and reduced glutaredoxins are very similar in stability. In heat-induced denaturation, monitored by CD, T_m is 55 and 57 °C for oxidized and reduced, respectively. In GuHCl denaturation, monitored by fluorescence, the midpoint denaturant concentrations are 2 M for both oxidized and reduced. It follows that the redox potentials of the disulfide bond are similar in unfolded and folded glutaredoxin. This is unexpected because in *E. coli* thioredoxin the oxidized form is far more stable than the reduced [Kelley, R. F., Shalongo, W., Jagannadham, M. V., & Stellwagen, E. (1987) *Biochemistry 26*, 1406–1411] and the redox potential of folded thioredoxin is significantly more negative than that of unfolded thioredoxin [Lin, T.-Y., & Kim, P. (1989) *Biochemistry 28*, 5282–5287].

Escherichia coli glutaredoxin is a small monomeric enzyme that catalyzes intracellular redox reactions by cyclic breakage and reformation of the disulfide bond between its active-site cysteines in the sequence -Cys-Pro-Tyr-Cys- (Fuchs, 1989; Holmgren, 1979a). It plays a central role in ribonucleotide reduction (Holmgren, 1976, 1979b; Kren et al., 1988) and sulfate reduction (Tsang, 1981; Kren et al., 1988). Glutaredoxin also has been shown to participate in reduction of methionine sulfoxide (Fuchs, 1977; Fuchs & Carlson, 1981) and protein disulfide linkages (Holmgren, 1979a).

Physical characterization of glutaredoxin has been limited by protein availability. We have cloned the gene for glutaredoxin and obtained abundant yields in an overexpression system. This permits us to undertake a study of glutaredoxin enzymology and folding thermodynamics, of which this is the first report. We are especially interested in comparisons between glutaredoxin and *E. coli* thioredoxin, a related redox protein with functional and structural similarity to glutaredoxin but with little sequence identity. *E. coli* thioredoxin (MW 11 700) contains a similar active-site sequence, -Cys-Gly-Pro-Cys-, and like glutaredoxin its only cysteine residues constitute the active site. Glutaredoxin is coupled to oxidation/reduction of glutathione, whereas thioredoxin redox activity is coupled to thioredoxin reductase. In both systems the

† This work is supported by grants from the University of Minnesota Industry–University Cooperative Research Center for Biocatalytic Processing, the University of Minnesota Graduate School, NIH GM40775 (for J.A.F. and B.K.), and NIH Molecular Biophysics Training Grant GM08277 (for V.A.S.).

* Author to whom correspondence should be addressed.

0006-2960/91/0430-5475$02.50/0

ultimate electron donor is NADPH[1] (Fuchs, 1989; Holmgren, 1979a).

The three-dimensional structure of *E. coli* glutaredoxin has not yet been experimentally determined, but it is expected to have a folding pattern common to the thioredoxin/glutaredoxin family (Eklund et al., 1984). A structure for glutaredoxin has been predicted by homologous modeling to the crystal structures of *E. coli* thioredoxin and T4 thioredoxin[2] (Eklund et al., 1984). Although thioredoxins and glutaredoxins have a common active-site motif of -Cys-X-X-Cys-, with a redox active disulfide between the two cysteines, *E. coli* glutaredoxin bears so little sequence similarity to *E. coli* thioredoxin that it was not clear that they have extensive tertiary homology until the structure of T4 thioredoxin was solved (Söderberg et al., 1978). T4 thioredoxin shares significant sequence homology with *E. coli* glutaredoxin. This provides a reliable secondary structure alignment from which glutaredoxin three-dimensional structure is modeled (Eklund et al., 1984).

The basic thioredoxin/glutaredoxin fold consists of a central β sheet of four or five strands, parallel except for one antiparallel strand, and three or four amphoteric helices. The helices connect strands of sheet, in a $\beta\alpha\beta$ arrangement, and pack against the sheet. Like T4 thioredoxin, *E. coli* glutaredoxin is expected to have a four-stranded central sheet packed by three helices. The -Cys-X-X-Cys- sequence is near the N terminus of a long helix in a $\beta\alpha\beta$ unit. Although the active-site residues are near the surface, all of one, and most of the second, cysteine side-chain atoms are buried.

In this paper we compare the folding/unfolding thermodynamics of oxidized (disulfide) and reduced (dithiol) glutaredoxin and thioredoxin. We find that reduced and oxidized glutaredoxin have very similar stabilities. This is in striking contrast to thioredoxin, for which the reduced form (trx-$(SH)_2$) is significantly less stable than the oxidized form (trx-S_2) (Kelley et al., 1987). The expected entropic effect of intrachain cross-linking is to stabilize the disulfide form relative to the dithiol. The structural basis for the absence of an increased stability of oxidized glutaredoxin over reduced glutaredoxin is not apparent. Circular dichroism spectra are very similar for folded oxidized and reduced glutaredoxin and are indistinguishable for denatured oxidized and reduced glutaredoxin. The similarity of the stabilities of oxidized and reduced glutaredoxin implies that the redox potentials of the disulfide group in folded and unfolded forms of glutaredoxin are about the same, whereas the redox potential of the disulfide group in folded thioredoxin is much more negative than in unfolded thioredoxin (Lin & Kim, 1989). Finally, the greater electrophoretic mobility of reduced glutaredoxin toward the anode at pH 7–8.5 indicates that the grx-$(SH)_2$ form has a greater negative charge, as would be expected if one or both cysteines have pK_a's lower than the normal pK_a of ~9. Surprisingly, thioredoxin, which is reported to have pK_a values of 6.7 and 9 for the active-site cysteine residues (Kallis & Holmgren, 1980), does not show a difference in electrophoretic mobility in the range pH 7–8.5.

Two *grx* gene products are obtained from our cloning system. To distinguish them we refer to the previously described glutaredoxin (85 amino acids in length; Höög et al., 1983) as glutaredoxin (grx) and the second, longer form of the enzyme as glutaredoxin N (grxN). GrxN differs from grx only in the N-terminal addition of the amino acid sequence Met-Arg-Arg-Glu-Ile-. Both glutaredoxins are encoded by the same gene, with translation of grxN commencing at a second in-frame start codon upstream of the previously identified AUG start site.

Materials and Methods

Reagents. Protein molecular weight standards were purchased from BRL Life Technologies, Inc. (BRL); restriction endonucleases and T4 DNA ligase were from Boehringer Mannheim Biochemicals; [^{35}S]methionine from Amersham; hydroxyethyl disulfide (HED) was from Aldrich Chemical Co. All reagents were of the highest grade available.

Recombinant DNA Materials and Techniques. Plasmids used were pBJF7 (Kren et al., 1988), pUC19 (Messing & Viera, 1982), pGP1-2, pT7-5 and pT7-6 (derivatives of pT7-1; Tabor & Richardson, 1985; S. Tabor, personal communication); strains were *E. coli* K-12 derivatives DH5a F′ (BRL), GM48 (this laboratory), and K38 (Russel & Model, 1984). Plasmids were isolated (Sambrook et al., 1989), and transformations were carried out as described by Mandel and Higa (1970) with minor modifications.

Construction of the Overexpression System. pBJF7 grown in the *dam*$^-$ host GM48 was digested with *Bcl*I and *Alu*I. The 425-bp fragment encoding glutaredoxin (Höög et al., 1986) was isolated by electroelution, cloned into pUC19 digested with *Bam*HI and *Sma*I, and transformed into DH5a F′. The resulting pUCgrx construct was digested with *Hin*cII and *Eco*RI, and the fragment encoding glutaredoxin was isolated by electroelution, cloned into both pT7-5 and pT7-6 digested with *Sma*I and *Eco*RI, and transformed into DH5a F′. This two-step construction creates a TAG stop codon in the polyclonal region 5′ to the ribosome binding site. Resulting glutaredoxin derivatives pT7-5grx and pT7-6grx and plasmids pT7-5 and pT7-6 were transformed into K38 containing pGP1-2. These four strains were grown in supplemented L broth (Höög et al., 1983) containing ampicillin (50 μg/mL) and kanamycin (40 μg/mL), centrifuged, and resuspended in cold, fully supplemented MOPS minimal medium (Niedhardt et al., 1974) lacking cysteine and methionine. Three aliquots from each culture were incubated for 1 h at 30 °C, and then two of the three aliquots for each construct were shifted to 42 °C to induce transcription of T7 RNA polymerase. After 15 min, rifampicin was added to one of each pair of temperature-shifted aliquots (200 μg/mL), and incubation continued at 42 °C for 10 min. The cultures were returned to 30 °C and incubated 20 min to allow decay of *E. coli* RNA polymerase-dependent mRNAs. [^{35}S]Methionine was added to all cultures (10 μCi/mL) 5 min before harvest. Crude extracts were electrophoresed by use of SDS–PAGE as described below, and proteins were visualized by autoradiography.

Glutaredoxin Purification. Growth of the engineered strain at 30 °C in TB media (Tartof & Hobbs, 1987) containing

[1] Abbreviations: grx, glutaredoxin (85 amino acids); grxN, glutaredoxin N (90 amino acids); grx-S_2 and grx-$(SH)_2$, oxidized and reduced forms of *E. coli* glutaredoxin, respectively; trx-S_2 and trx-$(SH)_2$, oxidized and reduced forms of *E. coli* thioredoxin, respectively; T4 trx-S_2 and T4 trx-$(SH)_2$, oxidized and reduced forms of thioredoxin from *E. coli* phage T4; BSA, bovine serum albumin; BPTI, bovine pancreatic trypsin inhibitor; DNA, deoxyribonucleic acid; DTT, dithiothreitol; GuHCl, guanidine hydrochloride; HED, hydroxyethyl disulfide; NADPH, β-nicotinamide adenine dinucleotide phosphate (reduced form); NEM, *N*-ethylmaleimide; PBS, phosphate-buffered saline; RNA, ribonucleic acid; SDS–PAGE, sodium dodecyl sulfate–polyacrylamide gel electrophoresis; TBS, Tris-buffered saline; CD, circular dichroism; NMR, nuclear magnetic resonance; FPLC, fast protein liquid chromatography; $\Delta G_{N\rightarrow D}$, free energy of a protein unfolding transition (native to denatured); $\Delta\Delta G_{ox\rightarrow red}$, difference in $\Delta G_{N\rightarrow D}$ between the oxidized and reduced forms of a protein.

[2] H. Eklund (personal communication) has proposed changing the name of T4 thioredoxin to T4 glutaredoxin because it shares greater functional and primary sequence similarity with the glutaredoxins than the thioredoxins.

ampicillin (50 μg/mL) and kanamycin (40 μg/mL) was followed by a temperature shift to 42 °C to initiate overproduction of glutaredoxin. After 15 min at 42 °C, rifampicin was added (100 μg/mL) and 10 min later the culture was brought down to 37 °C for 3 h. After centrifugation, the pellet was sonicated in buffer A (50 mM Tris-HCl, 1 mM EDTA, pH 8.0) containing protease inhibitors (0.1 μM pepstatin A and 0.5 mM phenylmethanesulfonyl fluoride) and the resulting crude extract was treated with streptomycin sulfate (0.8%) to precipitate nucleic acids. Glutaredoxin was isolated from filtered (0.22 μm) cell extract by use of size-exclusion chromatography (Sephadex G75, 5.2 cm × 115 cm column, eluted with buffer A) followed by anion-exchange chromatography (Mono Q, radial flow column or Pharmacia FPLC HR 5/5 column, eluted with a 0–0.5 M NaCl gradient in buffer A). Except for FPLC, which was conducted at room temperature, purification was carried out at 4 °C. The enzymatic activity of glutaredoxin (as GSH-disulfide transhydrogenase activity) was assayed with HED using the method of Holmgren (1985), with minor modifications (0.2 mM NADPH, 0.625 units/mL glutathione reductase). ΔA_{340} is linear up to a rate of 0.25 AU min^{-1}. SDS and native gel electrophoresis were used to assess protein purity. Glutaredoxin concentrations were determined by use of A_{280} and a molar extinction coefficient of 12 400 M^{-1} cm^{-1}. This value was determined from quantitative amino acid analysis and differs slightly from 11 600 M^{-1} cm^{-1} reported previously (Holmgren, 1979a). Total protein concentration in crude extracts were measured by use of the Bradford method (Bradford, 1976) (Bio-Rad, standard curve prepared from bovine serum IgG). Typically 20–30 g of cells was obtained from 10 L of culture, yielding 200–300 mg of glutaredoxin.

FPLC (Mono Q) was used to study equilibration among multiple grx conformers, conformational differences between oxidized and reduced grx, and effects of refolding on grx heterogeneity. In the equilibration experiments, grx as isolated (4.5 mg in 0.9 mL) was chromatographed and the heterogeneous region was divided into three fractions, desalted, and allowed to fully equilibrate. Aliquots (700 μg) from each fraction were then rechromatographed individually under identical conditions for comparison. In the oxidation/reduction experiments, several samples were analyzed: grx as isolated [which appears to be fully oxidized as it is not amenable to derivatization with *N*-ethylmaleimide (NEM)]; oxidized grx [10 mM oxidized dithiothreitol (DTT) in sample, 0.1 mM oxidized DTT in eluant]; reduced grx (10 mM DTT in sample, 0.1 mM DTT in eluant); and reoxidized grx (reduced in 10 mM DTT, desalted, reoxidized with 10 mM oxidized DTT in sample, 0.1 mM oxidized DTT in eluant). Comparisons were made by use of identical protein loads and concentrations (1.2 mg in 1.4 mL of buffer A). The redox state of grx was verified at each step by use of a simple gel-shift assay: samples were treated with NEM (five-fold molar excess over free sulfhydryl groups, pH 6.8) and then electrophoresed on pH 8.5 native gels. The mobility of derivatized grx is significantly retarded compared to oxidized grx. To determine whether unfolding followed by refolding eliminates the chromatographic heterogeneity characteristic of grx as isolated, FPLC was used to compare a renatured sample, prepared by extensively dialyzing unfolded grx (1.25 mg/mL in buffer A containing 3.5 M GuHCl) against buffer A at room temperature, with oxidized grx (as isolated) and reduced grx (1.2 mg protein, 0.95 mg/mL), using sample preparation and elution conditions described for the oxidation/reduction experiment. Elution profiles with identical heterogeneity patterns were observed for renatured grx and oxidized grx (as isolated), whereas the reduced protein produced a single peak (data not shown).

Electrophoresis. DNA fragments were electrophoresed on agarose gels in TBE (Sambrook et al., 1989). Proteins were electrophoresed on Tris/tricine polyacrylamide gels (native and SDS) by use of the method introduced by Schägger and von Jagow (1987) for small molecular weight proteins. Reduced samples were incubated for 15 min in 100 mM DTT. SDS samples were boiled for 4 min. SDS gels were treated with trichloroacetic acid prior to staining with Coomassie Blue R to wash away the detergent and precipitate the protein. Oxidized and reduced samples can be run on the same native gel provided they are separated by one empty lane.

Isoelectric focusing was carried out for 3.0 h on an LKB 2117 Multiphor II with LKB ampholine PAG plates, pH 4.0–5.0, cooled to 5 °C by a circulating water bath. Power supply upper limit settings were 1400 V, 50 mA, and 30 W. A gel strip was sliced into 1 cm × 0.5 cm squares, each square was suspended in 1 mL of water overnight at 4 °C, and the pH of each suspension was measured to establish the pH gradient.

Antibody Production and Western Blotting. Antibodies against *E. coli* grx were purified from chicken egg yolk (Jensenius et al., 1981; Gassman et al., 1990). Chickens inoculated with 100 μg of grx (0.5 mL, 1:5 PBS/Freund's complete adjuvant) were boosted with 50 μg of grx (0.5 mL, 1:3 PBS/Freund's incomplete adjuvant) at 4-week intervals. Anti-glutaredoxin was obtained from eggs produced during days 5–15 following the boosters.

Proteins electrophoresed on native gels were transferred to nitrocellulose by use of semidry electroblotting. The nitrocellulose support was blocked for 1 h with TBS/1% BSA/0.5% Tween 20/0.02% sodium azide, pH 7.5, probed overnight with anti-glutaredoxin in incubation buffer (identical with blocking buffer except that it contains 0.2% BSA), and then washed with incubation buffer (3 × 10 min). Incubation (1 h) with goat anti-chicken alkaline phosphate conjugate (0.2 μg/mL) (Bio-Rad) in incubation buffer was followed by additional washes with incubation buffer (3 × 10 min) and 0.1 M ethanolamine, pH 9.6 (1 × 10 min). Immunoreactions were visualized with 0.1 M ethanolamine/4 mM $MgCl_2$/0.1 mg/mL Nitro Blue Tetrazolium/60 μg/mL 5-bromo-4-chloro-3-indoyl phosphate. Polyclonal antibodies raised against *E. coli* grx cross-reacted with grxN but not T4 trx[2] or *E. coli* trx (data not shown).

Protein Composition and Sequence. Amino acid analysis of acid-hydrolyzed samples in Na S buffer (Beckman) was performed on a Beckman 6300 amino acid analyzer (25-cm column, Beckman Hi-Rez separation protocol). An Applied Biosystems, Inc. 470A protein sequenator with on-line PTH analysis was used for sequencing. N-Terminal sequences were confirmed by cleavage of grx and grxN in 70% formic acid with use of a 300-fold molar excess of CNBr (Holmgren & Reichard, 1967) and electrophoresis of reaction products on polyacrylamide gels (Laemmli, 1970) containing 6M urea but no SDS. Ion-spray mass spectrometry was performed on an ABI mass spectrometer in the laboratory of Dr. Larry Bowers.

Glutaredoxin in Vivo. In vivo degradation rates of grx and grxN were measured by use of pulse/chase experiments. Addition of [^{35}S]methionine to heat-induced cultures was followed by addition of nonradioactive methionine (1000-fold excess). Densitometric scans of autoradiograms prepared from native gels were used to calculate the relative amounts of grx and grxN in samples obtained at different time points. Relative distribution of grx and grxN between the cell pellet

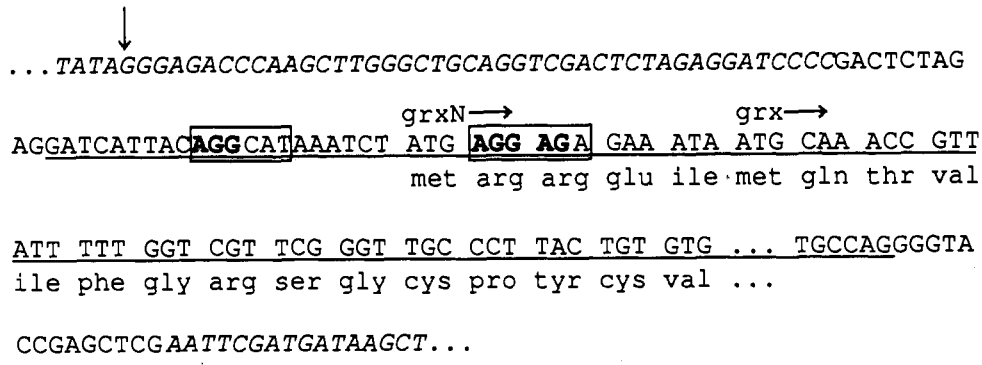

FIGURE 1: Partial sequence of pT7-6grx, the glutaredoxin overexpression construct: italics, fragments from pT7-6; plain text, fragments from pUC119; single underline, wild-type grx sequence; double underline, putative ribosome binding sites; bold, matches to Shine–Dalgarno consensus sequence; vertical arrow, putative mRNA start site in overexpression system (wild-type start site is farther upstream on the wild-type sequence, see text).

and crude extract was investigated by sonicating and centrifuging [^{35}S]methionine-labeled heat-induced cultures, dissolving the cell pellet in 10 M urea, electrophoresing the cell pellet and crude extract on native gels, and quantitating proteins densitometrically from autoradiograms.

Spectroscopic Measurements. Fluorescence measurements were made on a Perkin-Elmer MPF-44A fluorescence spectrophotometer; temperature was controlled with circulating water. Quantum yields were determined by comparing integrated tryptophan fluorescence intensity (0.75 μM in water) with that exhibited by grx samples (15–90 μg/mL in buffer A; reduced samples incubated for 15–45 min in 5–10 mM DTT, denatured samples in 4 M GuHCl). The independent effects of DTT and GuHCl on quantum yield were assessed by comparing the fluorescence intensity of free tryptophan in water with that exhibited by tryptophan samples containing DTT and/or GuHCl. An extinction coefficient of 5600 M^{-1} cm^{-1} and quantum yield of 0.144 was used for tryptophan in water (Wiget & Luisi, 1978).

Fluorescence intensity at 350 nm (λ_{max}) following excitation at 280 nm was used to monitor grx GuHCl denaturation. Small aliquots of 6M GuHCl were serially added to samples containing 80 μg of grx in buffer A (reduced samples contained 7–10 mM DTT), and emission intensity was recorded (1–3-min equilibration time). Values obtained from digitized spectra were normalized for protein concentration, and the fraction denatured was determined by normalizing against native and denatured base lines (Pace, 1986).

CD spectra were recorded on a Jasco J41C spectropolarimeter using water-jacketed cells of 1- or 0.1-mm path length. For thermal unfolding experiments, oxidized grx samples (0.1–0.4 mg/mL) were in 10 mM potassium phosphate, pH 7.0; reduced samples contained, in addition, 10 mM DTT and were allowed to stand for 15–30 min prior to analysis. To demonstrate reversibility, grx was subjected to a 25–80–25 °C cycle while θ_{220} was monitored; no hysteresis was observed. Thermal denaturation was monitored at θ_{220}; the fraction denatured was determined as described above.

RESULTS

Cloning, DNA Sequence Analysis, and Overexpression. The *E. coli BclI/AluI* fragment subcloned into pT7-6 contains the *grx* coding region plus an additional 36 bp upstream of the previously described (Höög et al., 1986) 5′ AUG translation initiation site (Figure 1). This upstream region contains a second in-frame AUG that would, if used as a translational start site, produce a glutaredoxin with five additional amino acids at the N terminus. Also present in this fragment is a second weak in-frame ribosome binding site appropriately located upstream from the second potential translation initiation site.

Table I: In Vivo Stability of Glutaredoxin[a]

	0[b]	15[b]	60[b]	120[b]
grxN	9.7 (100)	9.5 (98)	8.5 (88)	5.7 (59)
grx	42 (100)	38 (91)	37 (87)	24 (57)
grx:grxN	4:1	4:1	4:1	4:1

[a] Integrated peak intensities of autoradiogram bands; values in parentheses represent percent remaining relative to zero time. [b] Time after addition of nonradioactive methionine in minutes.

Glutaredoxin constitutes over 90% of total radiolabeled intracellular protein when induction at 42 °C is followed by addition of rifampicin to inhibit *E. coli* RNA polymerase activity. Both grx and grxN are present in the cell extract but are not distinguishable on ordinary 15% Laemmli gels since they both migrate with the dye front due to their small size (data not shown).

Identification and Characterization of Glutaredoxin N, a New Form of Glutaredoxin. After purification by standard chromatography (see Materials and Methods) a persistent minor band is clearly resolved on native gels at pH 8.5 (Figure 2a, lane 2) but not detectable on SDS gels (Figure 2b, lane 3). Anion-exchange FPLC (Mono Q, pH 8) with a shallow NaCl gradient permitted isolation of this material (peak 1, Figure 3b) which we subsequently characterized and named glutaredoxin N (grxN).

The amino acid composition of grxN is identical with grx with the addition of two arginines, one isoleucine, and one glutamic acid (methionines were not characterized). Edman analysis of the first 10 residues yields an N-terminal sequence of Met-Arg-Arg-Glu-Ile-Met-Gln-Thr-Val-Ile-, as predicted by the DNA sequence. The isoelectric points of grx and grxN are 4.6 and 4.9, respectively. Preliminary experiments suggest grxN is more active than grx and may be membrane associated; it is present in much higher proportion in the solubilized cell pellet. Grx and grxN both turn over in vivo on the hour time scale, and their turnover rates are similar (Table I). The ratio grx:grxN in crude extract from our overexpression system is approximately 4:1.

GrxN carries an additional positive charge between pH 5 and 11, which explains its slower migration on native gels at pH 8.5 (Figure 2a, lanes 3 and 4). Digestion of grxN with cyanogen bromide produces a fragment that comigrates with grx on a 6M urea gel at pH 8.5 (data not shown), indicating that the first five amino acids of grxN are removed during the digest since glutaredoxin does not contain any other methionines. In Western blots of native gels, grxN binds to chicken antibodies raised against grx.

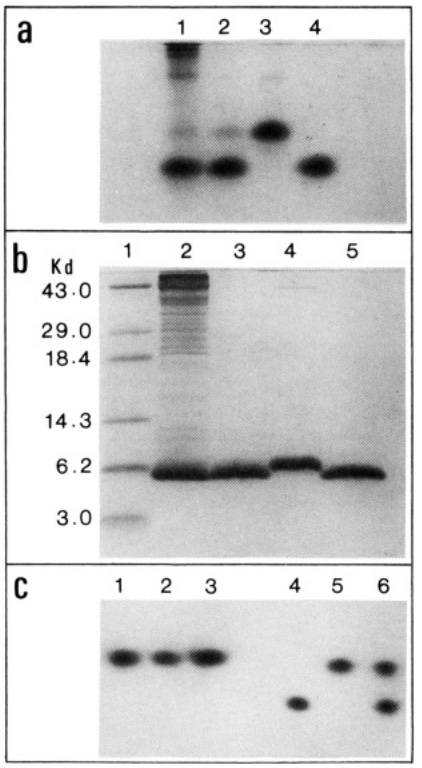

FIGURE 2: Gel electrophoresis of grx and grxN. (a) Native gel (pH 8.5, electrophoresis toward the anode): lane 1, crude cell extract; lane 2, active fraction before FPLC; lane 3, grxN after anion-exchange FPLC (peak 1 in Figure 3b); lane 4, grx after anion-exchange FPLC (peak region 2 in Figure 3b). (b) SDS gel: lane 1, molecular weight markers; lane 2, crude cell extract; lane 3, purified active fraction before FPLC; lane 4, grxN after anion-exchange FPLC (peak 1 in Figure 3b); lane 5, grx after anion-exchange FPLC (peak region 2 in Figure 3b). (c) Native gel (pH 8.5, electrophoresis toward the anode) comparing glutaredoxin and thioredoxin: lane 1, grx-S_2; lane 2, trx-S_2; lane 3, mixture of trx-S_2 and grx-S_2; lane 4, grx-$(SH)_2$; lane 5, trx-$(SH)_2$; lane 6, mixture of trx-$(SH)_2$ and grx-$(SH)_2$. The gel was preelectrophoresed with 50% (v/v) sodium thioglycolate (pH 9) in gel buffer to remove oxidants.

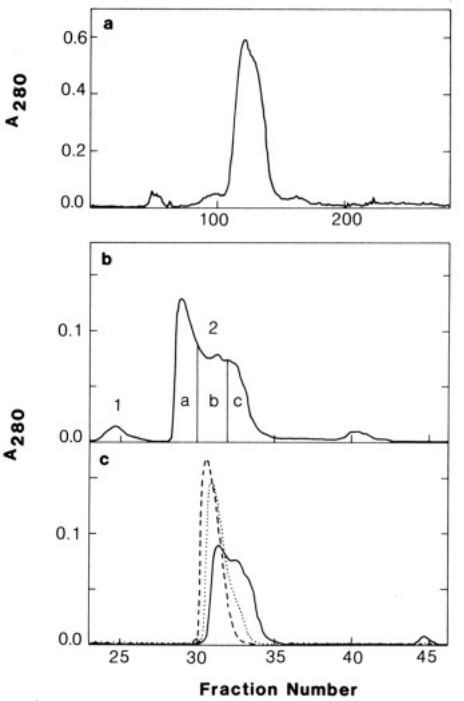

FIGURE 3: Anion-exchange chromatography of glutaredoxin. (a) Preparative scale radial flow (Q–Sepharose, 190 mg of protein, 10-mL fractions). (b) Preparative scale FPLC (Mono Q, 4.5 mg of protein, 1.0-mL fractions): peak 1, grxN; peak region 2, grx (areas a, b, and c within peak region 2 represent samples used in equilibration experiment; see text.) (c) FPLC oxidation/reduction experiment (1.2 mg of protein, 1.0-mL fractions): (—) oxidized grx as isolated, (– –) reduced grx, (···) grx reoxidized after in vitro reduction.

The small difference in molecular weight between grx (9700) and grxN (10 400) is discernible on high-resolution tricine/SDS gels where pure preparations of the proteins are run side by side (compare lanes 4 and 5, Figure 2b). Both glutaredoxins are unusual in that they migrate much faster than expected relative to molecular weight standards; they actually migrate faster than BPTI, a highly basic protein with MW 6200 (Figure 2b, lane 1). Recently, it was reported that deviations from expected mobilities on tricine/SDS gels correlate well with acid/base amino acid ratios (Huang & Matthews, 1990); acidic proteins (like grx) migrate substantially faster than basic proteins of the same molecular weight. In addition, grx and grxN may contain hydrophobic regions that cause exceptionally strong SDS binding, giving the proteins a higher mobility than expected. There are several indications that some part of the surface of glutaredoxin is unusually hydrophobic. For instance, efforts to purify glutaredoxin using hydrophobic chromatography failed due to tight binding of the protein to the resin (Pharmacia C12 Sepharose). Further, although their isoelectric points are identical (4.6), glutaredoxin elutes from DEAE columns significantly later in the NaCl gradient than *E. coli* thioredoxin, presumably due to nonspecific hydrophobic interactions of glutaredoxin with the DEAE resin. Also, in protein assays glutaredoxin binds Coomassie Blue to a greater extent than most other proteins, consistent with the existence of an unusually hydrophobic surface (Read & Northcote, 1981).

FPLC of Glutaredoxin. Glutaredoxin elutes from a standard Q–Sepharose column as a single peak (Figure 3a), yet it exhibits heterogeneity when chromatographed with use of anion-exchange FPLC (Figure 3b). Fractions a, b, and c, representing different regions of the grx elution profile (Figure 3b, peak 2) have identical quantitative amino acid compositions and identical electrophoretic behavior. The fractions retain their relative elution positions and shapes after salt removal and a lengthy equilibration period (data not shown). When oxidized grx is chemically denatured (6M GuHCl) and subsequently refolded, it elutes with an FPLC profile identical with the one obtained prior to denaturation (Figure 3c, solid line). However, the FPLC chromatographic heterogeneity in region 2 is eliminated by reduction and reoxidation (Figure 3b). The shoulders in peak 2 disappear when grx is reduced with DTT (Figure 3c). Reoxidation of reduced glutaredoxin after removal of the reducing agent results in a sharp peak with a faint shoulder. In addition, no suggestion of multiple shoulders is observed at lower protein load. Rechromatography after dialysis of small (50-μg) aliquots of fractions a, b, and c produces sharp peaks of indistinguishable elution times (data not shown). We conclude that the chromatographic differences between material in regions a, b, and c in peak 2 at high protein loads are due to subtle conformational differences in pure glutaredoxin, which may lead to differences in nonspecific hydrophobic interactions with the chromatographic resin.

Purity of Glutaredoxin. To insure that intact, bona fide glutaredoxin was obtained, its purity was rigorously demonstrated. First, multiple quantitative amino acid analyses give exactly the composition expected from the nucleotide sequence. Second, automated Edman degradation of the first 58 residues gives the expected sequence. Third, ion-spray mass spectrometry yields a monoisotopic mass of 9679.8, within two mass units of the calculated monoisotopic mass of 9677.8.

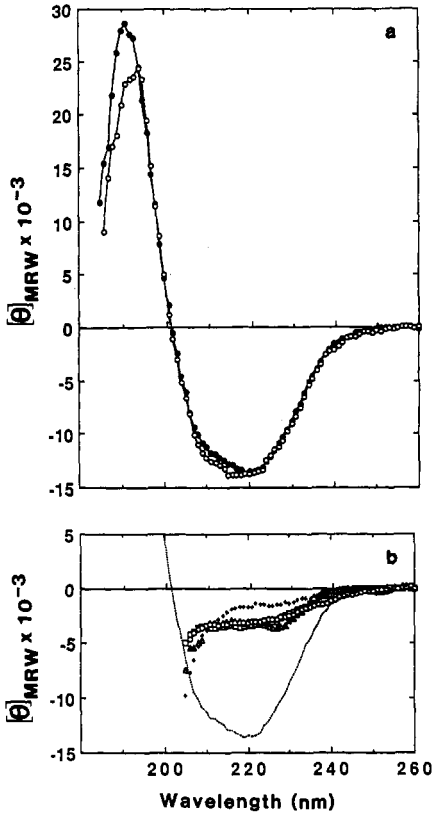

FIGURE 4: CD spectra of oxidized and reduced glutaredoxin. (a) Spectra at 25 °C, pH 8, for oxidized glutaredoxin (●) and reduced glutaredoxin (○). Mean residue ellipticity, $[\theta]_{MRW}$, for grx at pH 8 is −13 500 deg cm^2 dmol^{-1} at 220 nm. (b) Spectra at pH 8 of oxidized glutaredoxin at 70 °C (△), reduced glutaredoxin at 70 °C (□), oxidized glutaredoxin at 70 °C with 4 M GuHCl (○), and oxidized glutaredoxin at 25 °C with 4 M GuHCl (+). For reference, the spectrum of oxidized glutaredoxin from panel a is shown as a dotted line. The sample buffer is 5 mM Tris-HCl with 0.1 mM EDTA.

Further, our purified glutaredoxin is highly active enzymatically. In the transhydrogenase assay (described in Methods) our preparations have ~ 200 units/mg (μM NADPH oxidized min^{-1} mg^{-1} of protein), which compared very favorably to the specific activity reported previously (Holmgren, 1979a).

Circular Dichroism of Glutaredoxin. Circular dichroism spectra of folded oxidized and reduced grx are almost identical (Figure 4a). Similar CD spectra for oxidized and reduced glutaredoxin are in keeping with *E. coli* thioredoxin, which also show little difference between CD spectra of oxidized and reduced. The solution structure of reduced *E. coli* thioredoxin has been determined by NMR (Hiraoki et al., 1988; Dyson et al., 1989, 1990), and differences between reduced and oxidized are confined to the local vicinity of the active site. Crystal data has been obtained only for the oxidized *E. coli* thioredoxin (Holmgren et al., 1975; Katti et al., 1990) because reduced *E. coli* thioredoxin has not been suitably crystallized.

The CD spectra of thermally unfolded (70 °C) oxidized and reduced glutaredoxin are identical (Figure 4b). Addition of 4 M GuHCl to oxidized glutaredoxin at 70 °C does not alter its CD spectrum (Figure 4b). In 4 M GuHCl, the CD spectrum of oxidized glutaredoxin shows less ellipticity at 25 °C than at 70 °C. However, this does not imply increased structure at 70 °C (Privalov et al., 1989), as discussed below.

Fluorescence. Figure 5 shows fluorescence emission spectra of grx (oxidized and reduced, native and denatured) after excitation at 280 and 295 nm. For native grx, excitation at 295 nm, ordinarily specific for tryptophan (Schmid, 1989), produces almost no fluorescence (Figure 5a, lower curves). Excitation at 280 nm, affecting both tryptophan and tyrosine,

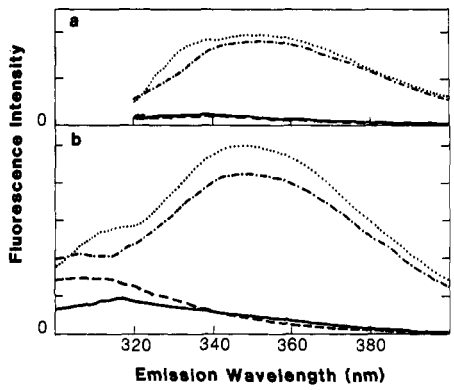

FIGURE 5: Fluorescence spectra of grx at 30 °C (19.4 μg/mL in 50 mM Tris-HCl/1 mM EDTA, pH 8.0, arbitrary intensity units): (—) native oxidized, (– –) native reduced (5 mM DTT), (·–·) denatured reduced (5 mM DTT, 4 M GuHCl), (···), denatured oxidized (4 M GuHCl); (a) excitation at 295 nm, (b) excitation at 280 nm.

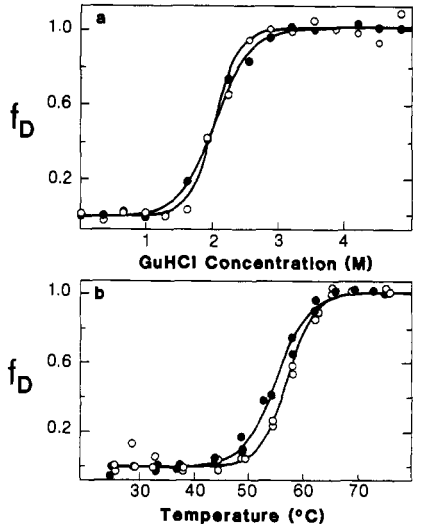

FIGURE 6: Glutaredoxin denaturation. (a) GuHCl denaturation followed by fluorescence (50 mM Tris-HCl/1 mM EDTA, pH 8.0). Samples were excited at 280 nm, and emission intensity at 350 nm (λ_{max}) was recorded; (●) grx-S_2; (○) grx-$(SH)_2$. (b) Thermal denaturation followed by CD at 220 nm (10 mM potassium phosphate, pH 7.0); (●) grx-S_2, (○) grx-$(SH)_2$.

produces a small amount of fluorescence at lower wavelengths. Fluorescence emission in folded glutaredoxin is not sensitive to the redox state except at lower wavelengths after excitation at 280 nm (Figure 5b, lower curves). In contrast to thioredoxin (Holmgren, 1972) the disulfide does not act as a tryptophan quenching agent.

Unfolded grx fluoresces when excited at both 280 and 295 nm but still exhibits low intensity (Figure 5a,b, upper curves). Interestingly, oxidized unfolded grx is more fluorescent than reduced unfolded grx. This difference is not attributable to static quenching by trace amounts of oxidized DTT (Sanyal et al., 1989); in control experiments DTT lowers the fluorescence intensity of free tryptophan by only 3.2% (1.6% in GuHCl), whereas the observed decrease in fluorescence for GuHCl-unfolded reduced vs oxidized grx is 16%.

Quantum yields for grx determined by comparison to tryptophan standards were 0.014 for native oxidized, 0.018 for native reduced, 0.083 for denatured oxidized, and 0.072 for denatured reduced forms.

Denaturation Experiments. GuHCl-induced unfolding was followed by the change in fluorescence intensity, and thermal unfolding of glutaredoxin was monitored by the change in CD ellipticity (Figure 6). Phosphate buffer (pH 7) was chosen

Table II: Thermodynamic Stability of Oxidized and Reduced Thioredoxins and Glutaredoxin

	GuHCl denaturation			thermal denaturation				
	C_m	ΔG(25 °C)[a]	ΔG(30 °C)	T_m	ΔH_m[a]	ΔG(25 °C)	ΔG(30 °C)	$\Delta\Delta G_{ox\rightarrow red}$(25 °C)
E. coli grx-S_2[b]	2.0		4.2	55	67	4.7	4.1	
E. coli grx-$(SH)_2$[b]	2.0		6.1	57	75	5.6	5.0	−0.9
E. coli trx-S_2[c]	2.6	8.6		86	104	9.4		
E. coli trx-$(SH)_2$[c]	1.8	6.2		75	84	6.2		3.2
T4 trx^2-S_2[d]	1.2-1.5	3.0-6.5						
T4 trx^2-$(SH)_2$[d]	0.9-1.1							

[a] ΔG and ΔH are in kilocalories per mole. [b] GuHCl denaturation is in 50 mM Tris-HCl/1 mM EDTA, pH 8, monitored by fluorescence; thermal denaturation is in 10 mM potassium phosphate, pH 7, monitored by CD at 220 nm. [c] GuHCl denaturation is in 50 mM phosphate, pH 7, monitored by fluorescence (Kelley et al., 1987); thermal denaturation is in 10 mM phosphate, pH 7, monitored by calorimetry (W. Bolen and M. Santoro, personal communication). [d] GuHCl denaturation is in 50 mM sodium phosphate, pH 6; a range of values is reported for CD and fluorescence measurements (Borden & Richards, 1990a,b).

for the CD experiments because of its low absorbance in the far-UV wavelength range; Tris buffer (pH 8) was used during purification and in all other experiments, including the thermal unfolding experiments, because cationic buffers are preferred for anion exchange chromatography.

Fluorescence at 350 nm following excitation at 280 nm at 30° was used to monitor GuHCl denaturation of oxidized and reduced grx (Figure 6a). Both forms denature at a concentration midpoint (C_m) of 2.0 M GuHCl, but calculated free energies of denaturation in the absence of GuHCl (assuming a two-state transition) were 4.2 kcal mol^{-1} for oxidized grx and 6.1 kcal mol^{-1} for reduced grx (Table II). The apparent difference in free energies reflects the values of m, the slope, describing the change in free energy as a function of [GuHCl]. For oxidized glutaredoxin, the data in Figure 6a give an m value of 2.1 kcal mol^{-1} M^{-1}; for reduced protein m = 3.4 kcal mol^{-1} M^{-1}.

Thermal denaturation of glutaredoxin followed by CD is shown in Figure 6b. The midpoint denaturation temperature, T_m, is 55 °C for grx-S_2 and 57 °C for grx-$(SH)_2$, and the change in enthalpy at T_m, ΔH_m, is 67 kcal mol^{-1} for grx-S_2 and 75 kcal mol^{-1} for grx-$(SH)_2$. Free energies of unfolding at temperature T, $\Delta G_{N\rightarrow D}(T)$, calculated from the experimental denaturation data (assuming a two-state transition and estimating ΔC_P as 12 cal mol^{-1} K^{-1} per amino acid residue) (Pace et al., 1989) are $\Delta G_{N\rightarrow D}$(25 °C) of 4.7 kcal mol^{-1} for grx-S_2 and $\Delta G_{N\rightarrow D}$(25 °C) of 5.6 kcal mol^{-1} for grx-$(SH)_2$ (Table II).

Differences in Charge Between Oxidized and Reduced Glutaredoxin. On native gels at pH 8.5, reduced grx moves much faster toward the anode than oxidized grx (Figure 2c, lanes 1 and 4). This implies that one or both cysteines are negatively charged at this pH. It is interesting that, under the same conditions, reduced and oxidized *E. coli* thioredoxin comigrate (Figure 2c, lanes 2 and 5) despite a report that the cysteine pK's are 6.7 and 9.0 (Kallis & Holmgren, 1980). It is not clear why thioredoxin gel mobility is inconsistent with the reported cysteine pK's.

Discussion

Glutaredoxin N. A new form of glutaredoxin, containing the additional N-terminal sequence Met-Arg-Arg-Glu-Ile-, has been isolated from a overproducing system of the cloned gene in *E. coli*. Pulse/chase experiments measuring the lifetimes of grxN and grx in vivo (Table I) indicate that grxN is not a precursor to grx because both proteins are degraded at the same rate. In crude extracts of overproducing cultures, grxN is at approximately 25% of the level of grx. The difference in expression level may reflect the relative strength of the Shine–Dalgarno (ribosome binding) sequences (Figure 1). The grxN:grx ratio is much lower in purified protein preparations, probably due to earlier elution of grxN from the anion-exchange columns.

The glutaredoxin mRNA produced by wild type *E. coli* contains an unusually long (179-bp) 5′ untranslated region (UTR) (B.K. and J.A.F., unpublished data). In contrast, the transcript present in our recombinant overproducing strain presumably contains only 75 bp upstream from the start site for grx, and of those only 36 are from the wild-type gene (Figure 1). The long 5′ UTR in the wild-type transcript may make possible posttranscriptional regulation of expression level and choice of start site. Further, efficiency of translation is known to be affected by RNA secondary structure (nucleotide base pairing) in the region of the initiation site (Munson et al., 1984; Gren, 1984). Computer-assisted modeling using the energy minimization algorithm of Zuker (1989) indicates regions of potential intrachain base pairing in the 5′ UTR of the wild-type transcript that would affect the environment of both ribosome binding sites and AUG start sites. Application of this algorithm to the putative mRNA produced in the overexpressing system, on the other hand, predicts little secondary structure formation; ribosome binding sites and translation initiation sites remain exposed (unpaired). This may explain why grxN is undetected in other systems but expressed to a significant extent in our pT7-6 construct.

Fully active N-terminal extended forms have been reported for a number of proteins, most of which are of viral origin (Kozak, 1986; Morel-Deville et al., 1990). Extended forms, though not common, are also known in bacteria. Recently, *E. coli* initiation factor IF2 was found to have two operational start sites (in this case, AUG and GUG), and the long and short gene products are produced in a 2:1 ratio (Morel-Deville et al., 1990). An earlier report describes two translation initiation sites for the chemotactic protein encoded by the *cheA* gene in *E. coli* and provides evidence of two gene products that differ only in the N-terminal extension of one predicted from the nucleotide sequence (Smith & Parkinson, 1980). The biological significance of two forms of these bacterial proteins is not clear. Im mammalian growth factors the N-terminal extension influences intracellular location of a protein. For example, Acland et al. (1990) report that the location of a mouse oncoprotein is determined by the presence of a 29 amino acid N-terminal extension, consistent with the general observation that N-terminal sequences direct protein trafficking within the cell and suggestive of important functional differences between the two forms. Future studies of grxN may reveal it to be a metabolically significant alternative form of glutaredoxin. Full characterization of its unique biological function, if any, will be aided by the construction of mutants that produce only grx or grxN, a project presently underway in our laboratories.

Secondary Structure. Two methods were used to predict

Table III: Protein Secondary Structure Predictions for Oxidized Glutaredoxin

	α helix	β sheet			β turn	random coil	total
		‖	anti-‖	total			
Chang et al.[a]	44			32	0	24	100
Manavalan and Johnson[b]	37	16	8	24	8	32	101
3D model[c]	36			24	13	27	100

[a] Calculated by use of the algorithm developed by Chang et al. (1978). [b] Calculated by use of the variable selection algorithm (Manavalan & Johnson, 1987) and extrapolation of ellipticity values between 184 and 185 nm. [c] Estimated from the three-dimensional structure predicted by modeling to the homologous proteins T4 thioredoxin[2] (Eklund et al., 1984; Söderberg et al., 1978) and *E. coli* thioredoxin (Katti et al., 1990).

secondary structure for folded grx from CD data (Table III). Like T4 thioredoxin and *E. coli* thioredoxin, *E. coli* glutaredoxin is expected to contain a high degree of α helix and β sheet (Eklund et al., 1984). Secondary structure percentages predicted with use of the "variable selection" method of Manavalan and Johnson (1987) compare very well with the secondary structure estimated from the alignment proposed by Eklund et al. (1984).

Steady-State Fluorescence of Glutaredoxin. Glutaredoxin is striking in its lack of fluorescence at 350 nm in the native state (Figure 5). The protein contains one tryptophan, Trp78, and four tyrosines, at residues 13, 33, 35, 72. Tyr13 is in the active-site disulfide loop, and Tyr33 is close to the disulfide in the three-dimensional structure modeled for *E. coli* glutaredoxin. The cause of Trp78 quenching is unclear; it cannot be the disulfide since the cysteine is located on the other side of the molecule. Nor is Trp78 quenched by a bound ligand, since glutaredoxin first unfolded in GuHCl and then refolded by removal of denaturant is still entirely quenched at 350 nm (data not shown). Since tryptophan fluorescence is effectively quenched in folded glutaredoxin, no indication of the hydrophobicity of the Trp78 local environment in native glutaredoxin can be surmised because λ_{max} cannot be determined.

Unlike *E. coli* thioredoxin, fluorescence of folded glutaredoxin is essentially unaffected by the redox state of the active-site disulfide. In *E. coli* thioredoxin, a large decrease in fluorescence intensity upon oxidation is generally thought to be due to quenching of Trp28 by the nearby disulfide. The small differences in oxidized vs reduced folded glutaredoxin fluorescence, observed below 330 nm after excitation at 280 nm (Figure 5b, lower curves), is probably due to effects on Tyr13 and Tyr33, which are near the active site.

When glutaredoxin is unfolded by GuHCl, fluorescence at 350 nm is observed, but at a very low intensity. Most denatured proteins have quantum yields in the range of 0.10–0.20 (Teale, 1960), while denatured glutaredoxin has a quantum yield of 0.08. Increased fluorescence intensity upon unfolding is not the common observation; unfolding ordinarily moves tryptophan residues from internal, hydrophobic environments, where fluorescence intensity is higher, into an aqueous environment that exerts a significant quenching effect. The observed increase in glutaredoxin fluorescence is presumably due to movement of the tryptophan away from a quenching group.

Relative Stability of Oxidized and Reduced Glutaredoxin: Comparisons to E. coli Thioredoxin. Despite the functional and conformational similarities of the disulfide environment in glutaredoxin and thioredoxin (Eklund et al. 1984), the presence of the disulfide bond markedly affects the thermodynamic stability of thioredoxin, but not glutaredoxin. Oxidized and reduced glutaredoxin have similar stabilities in thermal and GuHCl denaturation experiments (Table II). Our data suggest, moreover, that reduced glutaredoxin is somewhat more stable than oxidized. This is in marked contrast to thioredoxin, for which the oxidized form is 2–3 kcal mol^{-1} more stable than the reduced (Table II). The value of $\Delta G^\circ \cong 4$ kcal mol^{-1} is obtained for both thermal and GuHCl unfolding of oxidized glutaredoxin (Table II). The observed ΔG° for unfolding of reduced glutaredoxin is consistently 1–2 kcal mol^{-1} greater than for oxidized glutaredoxin, although the actual value is less certain.

The overall stability of glutaredoxin is much less than *E. coli* thioredoxin. At pH 7, grx-S_2 and grx-$(SH)_2$ have T_m's of 55 and 57 °C, respectively, while trx-S_2 and trx-$(SH)_2$ have T_m's of 86 and 75 °C (Table II).

Structural Origin of the Relative Stability Differences between Oxidized and Reduced Forms of Glutaredoxin and Thioredoxin. The CD data in Figure 4 indicate that oxidized and reduced glutaredoxin have essentially the same average secondary structure, whether folded or unfolded. There is little or no difference in CD spectra of oxidized and reduced folded glutaredoxin (Figure 4a). Likewise, unfolded glutaredoxin shows no CD difference between the two oxidation states (Figure 4b), but the interpretation requires a little more explanation: Around neutral pH, glutaredoxin is thermally unfolded at 70 °C and is chemically unfolded at 4 M GuHCl (Figure 6). CD spectra are indistinguishable for oxidized and reduced glutaredoxin at 70 °C. These spectra represent the fully denatured form of the protein, as demonstrated by the identical spectrum obtained for oxidized glutaredoxin at 70 °C with 4 M GuHCl added. The loss of ellipticity in oxidized glutaredoxin at 25 °C in 4 M GuHCl (Figure 4b) is similar to the behavior of a number of proteins as reported by Privalov et al. (1989). Privalov et al. attribute the CD spectrum at a high temperature in GuHCl to fully denatured protein. The decreased negative ellipticity in GuHCl at a lower temperature is apparently due either to temperature-dependent changes in protein secondary structure in GuHCl or to temperature-dependent changes of intrinsic spectral properties of the system unrelated to secondary structure (Privalov et al., 1989).

If the predominant effect of disulfide bond formation is its destabilization of the denatured state by reduction in configurational chain entropy, this ought to be reflected in the difference in the denaturation free energy, $\Delta\Delta G_{ox \rightarrow red}$, for the disulfide vs dithiol forms of the protein (Schellman, 1955; Thornton, 1981; Pace et al., 1988). The entropic contribution of a disulfide bond to protein stability can be estimated from statistical mechanics treatment of homopolymeric macrocyclization (Jacobson & Stockmayer, 1950; Flory, 1956; Poland & Scheraga, 1965). In its most useful form, this theory gives ΔS due to ring formation as a function of the number of residues in the ring, the spatial distribution of the monomers that form the connection (generally assumed to be a spherical Gaussian, which is not true for small chains), the volume element within which two residues must exist in order for the ring to form, and bond orientation (which may be favorable, neutral, or unfavorable depending on chain length). We have estimated the entropic contribution to the free energy of stabilization of the disulfide in the sequence -C-X-X-C- by two methods (Pace et al., 1988; Chan & Dill, 1989). Pace et al. (1988) modified an earlier approach of Schellman (1955), generating the expression $\Delta S = -2.1 - {}^3/_2 R \ln n$ (where n is the number of residues in the loop). For formation of a four-residue loop (-C-X-X-C-) at 25 °C, this translates into ΔG of 1.8 kcal mol^{-1}. Chan and Dill (1989) used computer simulation to study the effect of excluded volume on the entropy of loop formation, concluding that the power dependence

of ΔS on n is significantly greater than predicted by Jacobson and Stockmeyer (1950), especially for a loop in the middle of a long chain. Increasing the power dependence from $^3/_2$ to 2.4 (Chan & Dill, 1989) produces $\Delta S = -2.1 - 2.4R \ln n$, and the predicted $\Delta\Delta G_{ox\rightarrow red}$ for -C-X-X-C- is 2.6 kcal mol^{-1}, closer to the 3.2 kcal mol^{-1} reported for thioredoxin. Neither treatment takes into account bond directionality, which in the case of small chains is tied to the distribution function (Flory & Semlyen, 1966). The importance of bond directionality and distribution function is illustrated by experimental results for organic homopolymers showing that small ring (4–7 atoms) formation is much more likely and intermediate ring (10–16 atoms) formation much less likely than predicted by theory (Flory & Semlyen, 1966; Flory et al., 1976; Flory, 1988). The precise size range for loops whose ring formation is especially favored or disfavored depends on the nature of the homopolymer [most studies use poly(dimethylsiloxane)]. Nonetheless, it is interesting to note that the 14-membered ring in the -C-X-X-C- disulfide loop is of the size that seems to be less favored than predicted. Ring size might therefore exert a greater impact on the configurational entropy of the unfolded state containing the -C-X-X-C- motif than would otherwise be expected, perhaps even fully accounting for the $\Delta\Delta G_{ox\rightarrow red}$ exhibited by thioredoxin [cf. Hiraoki et al. (1988)].

In summary, current theory gives values for the entropic contribution of a disulfide in the sequence -C-X-X-C- to protein stability that compare reasonably with the value of $\Delta\Delta G_{ox\rightarrow red}$ for *E. coli* thioredoxin. However, this puzzle remains: why does glutaredoxin, which has the same -C-X-X-C- motif, not exhibit a similar value of $\Delta\Delta G_{ox\rightarrow red}$?

Part of the answer may lie in the extremely high β-turn potential (6.5×10^{-4}) for the glutaredoxin active site, -Cys-Pro-Tyr-Cys- (Chou & Fasman, 1978). In comparison, thioredoxin's -Cys-Gly-Pro-Cys- is a sequence with a strikingly low (Thornton, 1981) β-turn potential (5.5×10^{-5}). This does not necessarily suggest that glutaredoxin active-site sequence actually forms a β turn, since in both *E. coli* thioredoxin and T4 thioredoxin crystal structures the -Cys-X-X-Cys- active-site residues are the first four in a long helix. However, the favorability of a β turn in the sequence -Cys-Pro-Tyr-Cys- could contribute to more order in the average structure of reduced unfolded glutaredoxin.

Difference in Redox Potential between Folded and Unfolded Glutaredoxin. The fact that reduced and oxidized glutaredoxin have similar stabilities has interesting implications for the differences in redox potential between folded and unfolded glutaredoxin. Since both glutaredoxin and thioredoxin function in a disulfide/dithiol mechanism, the stabilities of the oxidized and reduced forms are linked to the redox potentials of the folded and unfolded forms by a thermodynamic cycle (Lin & Kim, 1989). The provocative result of this exercise for glutaredoxin is that the redox potentials of the folded and unfolded forms are nearly equal, with the folded form a little more positive. In contrast, the redox potential of folded thioredoxin, −260 mV (Holmgren, 1968), is much more negative than that of unfolded thioredoxin, approximately −180 mV, calculated from data reported by Lin and Kim (1989).

ACKNOWLEDGMENTS

We thank Dr. Hans Eklund for access to thioredoxin and glutaredoxin coordinates and for helpful discussions, Dr. Stan Tabor for kindly providing us with the T7 expression system, and Ms. Lori Anderson for assistance in the purification of glutaredoxin. Computer facilities for this work were provided by the Molecular Biology Computer Center for the University of Minnesota.

REFERENCES

Acland, P., Dixon, M., Peters, G., & Dickson, C. (1990) *Nature 343*, 662–665.
Borden, K. L. B., & Richards, F. M. (1990a) *Biochemistry 29*, 3071–3077.
Borden, K. L. B., & Richards, F. M. (1990b) *Biochemistry 29*, 8207–8210.
Bradford, M. (1976) *Anal. Biochem. 72*, 248–254.
Chan, H. S., & Dill, K. A. (1989) *J. Chem. Phys. 90*, 492–509.
Chou, P. Y., & Fasman, G. D. (1978) *Adv. Enzymol. Relat. Areas Mol. Biol. 47*, 45–148.
Dyson, H. J., Holmgren, A., & Wright, P. E. (1989) *Biochemistry 28*, 7074–7087.
Dyson, H. J., Gippert, G. P., Case, D. A., Holmgren, A., & Wright, P. E. (1990) *Biochemistry 29*, 4129–4136.
Eklund, H., Cambillau, C., Sjöberg, B.-M., Holmgren, A., Jörnvall, H., Höög, J.-O., & Brändén, C.-I. (1984) *EMBO J. 3*, 1443–1449.
Flory, P. J. (1956) *J. Am. Chem. Soc. 78*, 5222–5235.
Flory, P. J. (1988) *Statistical Mechanics of Chain Molecules*, pp 392–396, Hanser Publishers, New York.
Flory, P. J., & Semlyen, J. A. (1966) *J. Am. Chem. Soc. 88*, 3209–3212.
Flory, P. J., Suter, U. W., & Mutter, M. (1976) *J. Am. Chem. Soc. 98*, 5733–5739.
Fuchs, J. A. (1977) *J. Bacteriol. 129*, 967–972.
Fuchs, J. A. (1989) in *Glutaredoxin and Glutathione: Chemical, Biochemical, and Medical Aspects, Part B* (Dolphin, D., Poulson, R., & Avramovic, O., Eds.) pp 551–570, John Wiley & Sons, Inc., New York.
Fuchs, J. A., & Carlson, J. (1981) in *Thioredoxins: Structure and Functions* (Gadal, P., Ed.) pp 111–118, National Center for Scientific Research, Paris.
Gassman, M., Thömmes, P., Weiser, T., & Hübscher, U. (1990) *FASEB J. 4*, 2528–2532.
Gren, E. J. (1984) *Biochimie 66*, 1–29.
Hiraoki. T., Brown, S. B., Stevenson, K. J., & Vogel, H. J. (1988) *Biochemistry 27*, 5000–5008.
Holmgren, A. (1968) *Eur. J. Biochem. 6*, 475–484.
Holmgren, A. (1972) *J. Biol. Chem. 247*, 1992–1998.
Holmgren, A. (1976) *Proc. Natl. Acad. Sci. U.S.A. 73*, 2275–2279.
Holmgren, A. (1979a) *J. Biol. Chem. 254*, 3664–3671.
Holmgren, A. (1979b) *J. Biol. Chem. 254*, 3672–3678.
Holmgren, A. (1985) *Methods Enzymol. 113*, 525–540.
Holmgren, A., & Reichard, P. (1967) *Eur. J. Biochem. 2*, 187–196.
Holmgren, A., Söderberg, B.-O., Eklund, H., & Brändén, C.-I. (1975) *Proc. Natl. Acad. Sci. U.S.A. 72*, 2305–2309.
Höög, J.-O., Jörnvall, H., Holmgren, A., Carlquist, M., & Persson, M. (1983) *Eur. J. Biochem. 136*, 223–232.
Höög, J.-O., von Bahr-Lindström, H., Jörnvall, H., & Holmgren, A. (1986) *Gene 43*, 13–21.
Huang, J., & Matthews, H. R. (1990) *Anal. Biochem. 188*, 114–117.
Jacobson, H., & Stockmayer, W. H. (1950) *J. Chem. Phys. 18*, 1600–1606.
Jensenius, J. C., Andersen, I., Hau, J., Crone, M., & Koch, C. (1981) *J. Immunol. Methods 46*, 63–68.
Kallis, G.-B., & Holmgren, A. (1980) *J. Biol. Chem. 255*, 10261–10265.
Katti, S. K., LeMaster, D. M., & Eklund, H. (1990) *J. Mol. Biol. 212*, 167–184.
Kelley, R. F., Shalongo, W., Jagannadham, M. V., & Stellwagen, E. (1987) *Biochemistry 26*, 1406–1411.

Kozak, M. (1986) *Cell 47*, 481-483.
Kren, B., Parsell, D., & Fuchs, J. A. (1988) *J. Bacteriol. 170*, 308-315.
Laemmli, U. K. (1970) *Nature 227*, 680-685.
LeMaster, D. (1986) *J. Virol. 59*, 759-760.
Lin, T.-Y., & Kim, P. S. (1989) *Biochemistry 28*, 5282-5287.
Manavalan, P., & Johnson, W. C., Jr. (1987) *Anal. Biochem. 167*, 76-85.
Mandel, M., & Higa, A. (1970) *J. Mol. Biol. 53*, 159-162.
Messing, J., & Vieira, J. (1982) *Gene 19*, 269-276.
Morel-Deville, F., Vachon, G., Sacerdot, C., Cozonne, A. J., Grunberg-Manago, M., & Cenatiempo, Y. (1990) *Eur. J. Biochem. 188*, 605-614.
Munson, J. M., Stormo, G. D., Niece, R. L., & Reznikoff, W. S. (1984) *J. Mol. Biol. 177*, 663-683.
Mutter, M. (1977) *J. Am. Chem. Soc. 99*, 8307-8314.
Pace, C. N. (1986) *Methods Enzymol. 131*, 266-280.
Pace, C. N., Grimsley, G. R., Thomson, J. A., & Barnett, B. J. (1988) *J. Biol. Chem. 263*, 11820-11825.
Pace, C. N., Shirley, B. A., & Thomson, J. A. (1989) in *Protein Structure: A Practical Approach*, (Creighton, T. E., Ed.) pp 311-330, IRL Press, New York.
Poland, D. C., & Scheraga, H. A. (1965) *Biopolymers 3*, 379-399.
Privalov, P., Tiktopulo, E., Venyaminov, S., Griko, Yu., Makhatadze, G., & Khechinashvili, N. (1989) *J. Mol. Biol. 205*, 737-750.
Read, S. M., & Northcote, D. H. (1981) *Anal. Biochem. 116*, 53-64.
Russel, M., & Model P. (1984) *J. Bacteriol. 159*, 1034-1039.
Sambrook, J., Fritsch, E. F. & Maniatis, T. (1989) *Molecular Cloning: A Laboratory Manual*, 2nd Ed., Cold Spring Harbor Laboratory Press, Cold Spring Harbor, NY.
Sanyal, G., Kim, E., Thompson, F. M., & Brady, E. K. (1989) *Biochem. Biophys. Res. Commun. 165*, 772-781.
Schägger, H., & von Jagow, G. (1987) *Anal. Biochem. 166*, 368-379.
Schellman, J. A. (1955) *C. R. Trav. Lab. Carlsberg, Ser. Chim. 29*, 230-259.
Schmid, F. X. (1989) in *Protein Structure: A Practical Approach*, (Creighton, T. E., Ed.) pp 251-285, IRL Press, New York.
Smith, R. A., & Parkinson, J. S. (1980) *Proc. Natl. Acad. Sci. U.S.A. 77*, 5370-5374.
Söderberg, B.-O., Sjöberg, B.-M., Sonnerstam, U., & Brändén, C.-I. (1978) *Proc. Natl. Acad. Sci. U.S.A. 75*, 5827-5830.
Tabor, S., & Richardson, C. C. (1985) *Proc. Natl. Acad. Sci. U.S.A. 82*, 1074-1078.
Tartof, K. D., & Hobbs, C. A. (1987) *Focus 9* (2), 12.
Teale, F. W. J. (1960) *Biochem. J. 76*, 381-388.
Thornton, J. M. (1981) *J. Mol. Biol. 151*, 261-287.
Tsang, M. L.-S. (1981) *J. Bacteriol. 146*, 1059-1066.
Wiget, P., & Luisi, P. L. (1978) *Biopolymers 17*, 167-180.
Zuker, M. (1989) *Methods Enzymol. 180*, 262-288.

Solution Structure of Human Insulin-Like Growth Factor 1: A Nuclear Magnetic Resonance and Restrained Molecular Dynamics Study[†,‡]

Robert M. Cooke,[§] Timothy S. Harvey, and Iain D. Campbell*
Department of Biochemistry, University of Oxford, South Parks Road, Oxford OX1 3QU, U.K.
Received November 14, 1990; Revised Manuscript Received February 8, 1991

ABSTRACT: The solution structure of human insulin-like growth factor 1 has been investigated with a combination of nuclear magnetic resonance and restrained molecular dynamics methods. The results show that the solution structure is similar to that of insulin, but minor differences exist. The regions homologous to insulin are well-defined, while the remainder of the molecule exhibits greater disorder. The resultant structures have been used to visualize the sites for interaction with a number of physiologically important proteins.

Over recent years the requirement of protein growth factors for the control of cell growth and replication has become increasingly apparent, and the number of growth factors known to exist has multiplied dramatically. Most of these proteins are thought to act by binding to cell-surface receptors and activating intracellular tyrosine kinases [reviewed by Yarden and Ullrich (1988)]. Attempts have been made to subdivide the growth factors on the basis of sequence homologies (James & Bradshaw, 1984), and such consideration revealed that one group closely resembled insulin, prompting their renaming as insulin-like growth factors (IGFs)[1] (Rinderknecht & Humbel, 1976). Two distinct IGFs have been found in many mammalian species: IGF-1, the human form of which is also known as somatomedin C (Daughaday et al., 1972), and IGF-2, which was known as multiplication-stimulating activity (Dulak & Temin, 1973). The IGFs are also thought to be responsible for the nonsuppressible insulin-like activity observed in serum (Froesch et al., 1963).

[†] Supported by grants from the Monsanto Chemical Company, ICI Pharmaceuticals, and the Science and Engineering Research Council.
* Author to whom correspondence should be addressed.
[‡] The coordinates for the structures in this paper have been deposited with the Brookhaven Protein Database.
[§] Current address: Glaxo Group Research Greenford Road, Greenford, Middlesex UB6 0HE, U.K.

[1] Abbreviations: IGF-1, insulin-like growth factor 1; NMR, nuclear magnetic resonance; RMD, restrained molecular dynamics; IGF-2, insulin-like growth factor 2; TPPI, time-proportional phase incrementation; COSY, correlated spectroscopy; DQF-COSY, double-quantum filtered correlated spectroscopy; NOESY, nuclear Overhauser effect spectroscopy; TOCSY, total correlation spectroscopy.

0006-2960/91/0430-5484$02.50/0